J. King Saud Univ., Vol. 14, *Eng. Sci.* (1), pp. 41-52, Riyadh (1422/2002)

Energy Projection in Polynomial Correlation Filters

Khalid A. Al-Mashouq[*], B. V. K. Vijaya Kumar[**] and Mohamed Alkanhal[**]

[*]*Electrical Engineering Department, King Saud University*
PO Box 800, Riyadh 11421, Saudi Arabia
Email: mashouq@ksu.edu.sa

[**]*ECE Department, Carnegie Mellon University, Pittsburgh, PA 15213, USA*

(Received 05 June 2000; accepted for publication 16 December, 2000)

Abstract. In this paper we present a new version of the polynomial correlation filter (PCF) called constrained polynomial correlation filter (CPCF). We investigate the performance of this filter in the presence of clutter noise. The peak-to-sidelobe ratio measure is evaluated for public MSTAR images. The effect of different terms in the polynomial filter is examined by simulation. Then, we introduce a theoretical framework called energy projection to predict the effectiveness of different terms in the CPCF.

Keywords: Polynomial filter, correlation filter, CPCF, nonlinear filter, MSTAR.

Introduction

Correlation filters are 2-D spatial filters used to detect, locate and classify targets observed in noisy scenes [1-8]. A good filter should yield sharp correlation peaks for targets of interest, high discrimination against clutter and high tolerance to distortion in the target. To meet these desired criteria, several filters have been introduced in the past. A tutorial survey paper by Kumar [1] reviews many of these filters.

Correlation filters are linear by nature, since their implementation relies on the computational efficiency of the 2-D FFT. However, we can still utilize the computational advantage of the FFT if we perform "restricted" nonlinearity on the input scene. Recently, Mahalanobis and Kumar [9] proposed a new nonlinear correlation filter architecture called polynomial correlation filter (PCF) for correlation-based pattern recognition. The input to this filter is the original scene and its point-by-point n^{th} orders, where n is an integer. They derived a closed-form solution for the PCF. Preliminary simulations demonstrated that this type of filters can provide significant improvement in the peak-to-sidelobe ratio (PSR) compared to its linear counterparts.

Here, we wish to investigate the performance of PCF in the presence of background clutter. As mentioned above, the filter performance is measured by high correlation peaks for targets and low correlation values for clutter. To make the analysis more tractable, we introduce a modified PCF called constrained polynomial correlation filter (CPCF). The main objective of this filter is maintaining the correlation peaks due to targets fixed for all polynomial filters. This makes the comparison between different filters easier since we need to compare only the filter's response due to clutter. No attempt has been made in this paper to compare PCF with CPCF.

To predict the performance of CPCF, we propose a method called energy projection which depends on some linear algebra tools. Our attention here is on CPCF's which use polynomials of the form $x+x^n$, where n is an integer. We expect that this method can be generalized to predict the performance of wider range of nonlinear correlation filters. We study the effect of varying n on the clutter PSR. We also predict the performance of the CPCF as n approaches infinity. To verify this method we perform many simulations using the public MSTAR database.

The organization of this paper is as follows. In the next section, we present the theory of CPCF. Then we evaluate the CPCF using images from the public MSTAR. Finally we present the energy projection method which is used to analyze and explain the simulation results.

Constrained Polynomial Filter

In this paper, we will use the following notation: images are expressed as column vectors $\mathbf{x}$ by lexicographical scanning and $\mathbf{x}^j$ represents the vector $\mathbf{x}$ with each of its elements raised to the power j. The complex conjugate transpose is represented by the superscript $^+$. Matrices are represented by upper case characters. All filters, images and output in this section are represented in frequency domain.

For simplicity, we will derive the second order polynomial filter which can be easily generalized to any other higher order. Our objective is to find the two filters, $\mathbf{h}_1$ and $\mathbf{h}_2$, where the input to these filters is $\mathbf{x}$ and $\mathbf{x}^2$, respectively.

Like any other constrained filter design, it is required to have a constraint c_i at the output origin due to i^{th} training image, $\mathbf{x}_i$, or

$$\mathbf{h}_1^+\mathbf{x}_i^1 + \mathbf{h}_2^+\mathbf{x}_i^2 = c_i \tag{1}$$

This equation can be rewritten as:

$$\begin{bmatrix} \mathbf{h}_1^+ & \mathbf{h}_2^+ \end{bmatrix} \begin{bmatrix} \mathbf{x}_i^1 \\ \mathbf{x}_i^2 \end{bmatrix} = c_i \tag{2}$$

We can define a block matrix **R** as:

$$\mathbf{R} = [\mathbf{r}_1 \quad \mathbf{r}_2 \quad \ldots \quad \mathbf{r}_N] \tag{3}$$

where

$$\mathbf{r}_i = \begin{bmatrix} \mathbf{x}_i^1 \\ \mathbf{x}_i^2 \end{bmatrix} \tag{4}$$

For the block matrix **R,** the constraints in Eq. (2) can be rewritten as follows:

$$\mathbf{R}^+\mathbf{h} = \mathbf{c}^* \tag{5}$$

where

$$\mathbf{c} = [c_1 \quad \ldots \quad c_N]^T \tag{6}$$

and

$$\mathbf{h} = \begin{bmatrix} \mathbf{h}_1 \\ \mathbf{h}_2 \end{bmatrix} \tag{7}$$

Here, we will work on the average similarity measure, ASM, metric which can be easily replaced by any other metric. From the PCF paper [9], we can define the ASM as:

$$\mathbf{ASM} = \mathbf{h}_1^+\mathbf{S}_{11}\mathbf{h}_1 + \mathbf{h}_1^+\mathbf{S}_{12}\mathbf{h}_2 + \mathbf{h}_2^+\mathbf{S}_{21}\mathbf{h}_1 + \mathbf{h}_2^+\mathbf{S}_{22}\mathbf{h}_2 \tag{8}$$

This can be rewritten as:

$$\mathbf{ASM} = \mathbf{h}^+\,\mathbf{Sh} \tag{9}$$

where

$$\mathbf{S} = \begin{bmatrix} \mathbf{S}_{11} & \mathbf{S}_{12} \\ \mathbf{S}_{21} & \mathbf{S}_{22} \end{bmatrix} \tag{10}$$

where $\mathbf{S}_{11}$, $\mathbf{S}_{12}$, $\mathbf{S}_{21}$ and $\mathbf{S}_{22}$ are all diagonal matrices. Minimizing the ASM in Eq. (9) subject to the constraints in Eq. (5) leads to the well-known solution:

$$\mathbf{h} = \mathbf{S}^{-1}\mathbf{R}\left(\mathbf{R}^{+}\mathbf{S}^{-1}\mathbf{R}\right)^{-1}\mathbf{c}^{*} \tag{11}$$

Performance of CPCF on Public MSTAR Images

The CPCF derived above is examined using the public domain MSTAR database. Our simulation is carried out on the 232 images of T72 with serial number SN_132. Figure 1 shows samples of the T72 images. The number of aspect bins is selected to be 12. The images are grouped according to the nearest aspect bin. The group of images in each aspect bin is used to build a CPCF filter. To test the filter response to clutter, we chipped out 539 clutter images from the clutter set. Equation (11) is used to find **h** for different polynomial filters of the form $x+x^n$, where n takes on the values 2, 3, 4, 5 and 6. The peak to sidelobe ratio (PSR) of the filter output defined as

$$\mathrm{PSR} = \frac{\text{peak} - \text{mean}}{\text{standard deviation}} = \frac{p - \mu}{\sigma}$$

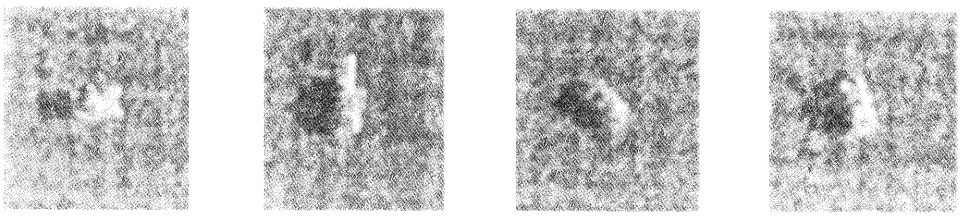

Fig. 1. Sample T72 images from MSTAR database.

was computed and used for evaluating the performance of each filter. For testing, we used the same training images. Then we tested the filters with the clutter scenes. In both cases, we computed the PSR. Figure 2 shows the PSR for target scenes (upper curve) and for clutter scenes (lower curve) corresponding to CPCF filters of the form $x+x^n$, with n=2,3,4, 5 and 6. We did not show the PSR curves for higher order filters because we found out that they all almost replicate the curves of the $x+x^6$ filter. For reference, we also include the result of the (linear) MACH filter [4] on the same figure. From this figure, one can see that the CPCF helps reduce the PSR of the clutter. In addition, we notice the similarity between the signal PSR of different CPCF. This is due to the design criterion (constrained output) used in designing the CPCF. Therefore, we may now restrict our attention to the behavior of CPCF with clutter images. For comparison purpose, we computed the PSR variance of the clutter for the five CPCF's considered here. This variance is depicted in Figure 3. In the next section, we analyze these results

and attempt establishing a theoretical framework that can be useful in analyzing and predicting the behavior of CPCF.

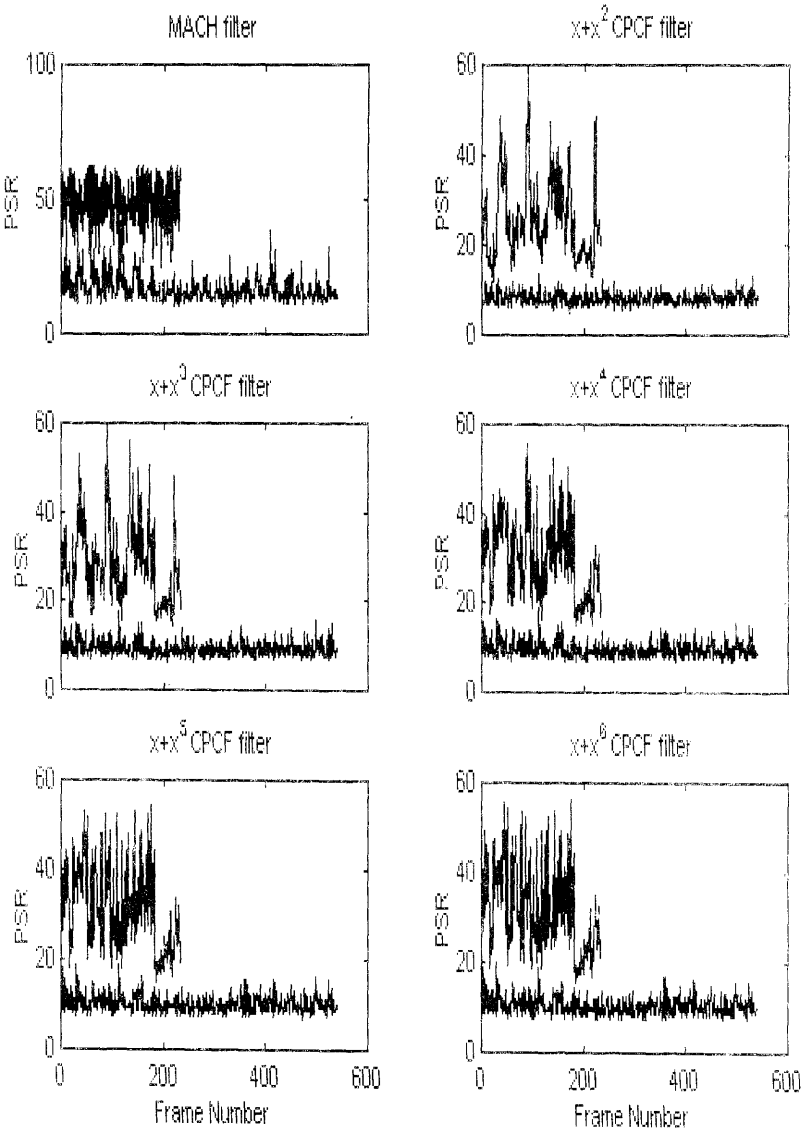

Fig. 2. PSR evaluated for different filters. On each graph, the upper curve represents the PSR due to target scenes, and the lower curve represents the PSR due to clutter.

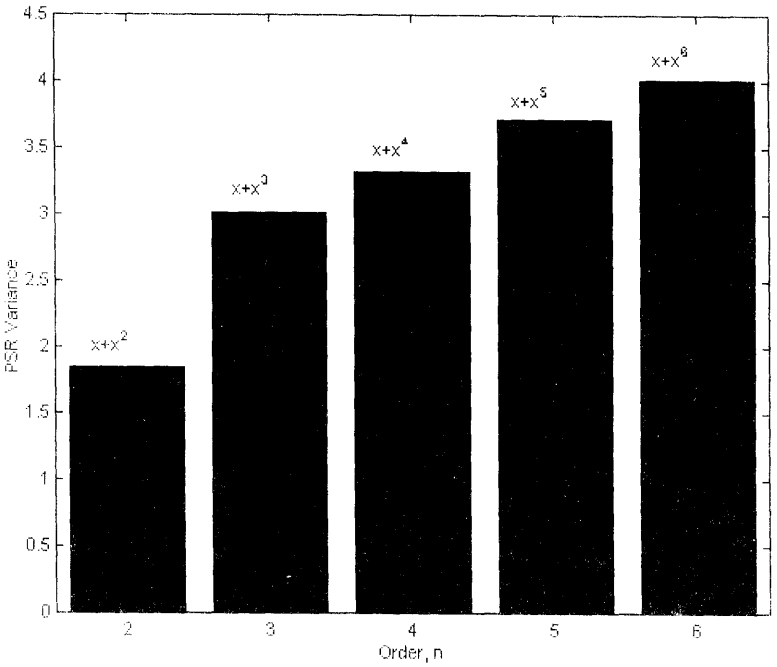

Fig. 3. Psr variance due to clutter scenes for different cpcf's.

Analysis and Discussion

The polynomial filter can be viewed as a multi-sensor system, where the input to the detector is images taken from different sensors. However, here the additional image copies are obtained by processing the original image through some nonlinear functions. Note that any linear transformation of the image is not useful since it can be incorporated in one (linear) filter. By generating nonlinearly transformed images, we hope that the target correlation from the different images will add up coherently, while the clutter correlation will add up noncoherently.

In the simulations presented in the previous section, we consider point-by-point nonlinear transformation of the form x^n. Therefore, the input to the CPCF filter is a pair of images, x and x^n. The optimization procedure used in deriving Eq. (11) will result in h_2 that is proportional to the significance of information in x^n. In the extreme case where x^n provides no new information, h_2 will be set to zero. In this case, the performance of the CPCF is equivalent to the performance of its linear counterpart.

To investigate the contribution of the second filter, $\mathbf{h}_2$, we perform the following experiment. We evaluate the contribution of the second filter to the peak output for target scenes. The output of the second filter is divided by the total output. This is averaged over all target scenes and displayed in Fig. 4. This figure shows that the contribution of the second filter starts at more than 20% of the total output for n=2. As n gets larger, the contribution of $\mathbf{h}_2$ becomes smaller to reach only 5% for n=6. As n approaches infinity the contribution will reach zero, in a negative-exponential-like manner, and the CPCF becomes equivalent to a linear one. We recommend here that the use of CPCF should be restricted to the first significant few terms.

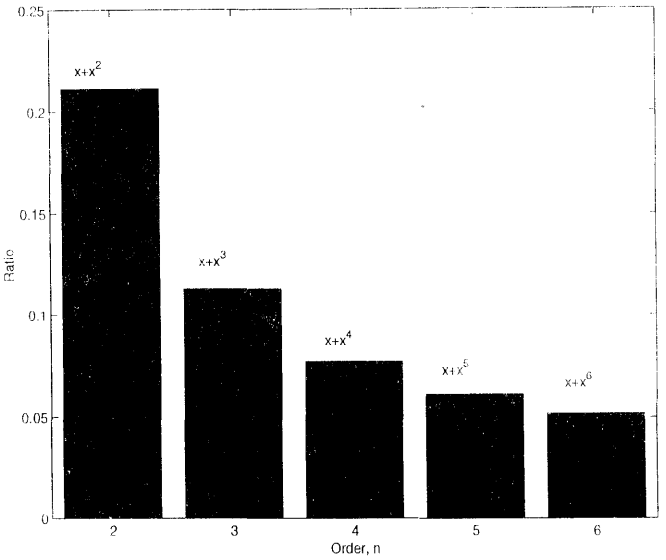

Fig. 4. Contribution of the second filter to the peak output relative to the total.

The result shown in Figure 4 can also be used to explain the clutter PSR variance in Figure 3. Another way to assess the contribution of a second filter in CPCF is to look at the signal PSR relative to the clutter PSR. Since the signal PSR is almost fixed, a good filter should reduce the clutter PSR. When there is significant contribution from the second filter, it should help reduce the PSR of the clutter. Comparing the bar graphs in Figs. 3 and 4, we found that they complement each other; high peak contribution leads to low clutter PSR variance and vice versa.

What happens when we raise the image, pixel-by-pixel, to the n^{th} power? Consider two pixels, with values a and b, where a>b. Raising each one to the n^{th} power will make the second pixel relative to the first one b^n/a^n. If a is the highest value in the image, then

all pixels with lower values will be reduced. If n gets very large then all points are suppressed except the peak values. In frequency domain, raising an image to the n^{th} power is equivalent to n-1 convolutions. Several convolutions result in broadening the image in frequency domain. This translates to sharp spikes in the spatial domain. Usually an image has only small number of peaks, which will dominate the scene. In effect, raising an image to the n^{th} power results in a scene with smaller target (after normalization.) Experience shows that the performance degrades with smaller targets.

The argument presented above, although plausible, does not address the linear dependency between images. To have better insight into this important issue, we present the following framework based on linear algebra basics [10,11]. Consider the vector subspace, χ, spanned by the set of all training images (in one aspect bin.) We perform Gram Schmidt orthogonalization procedure [10,11] on all images in χ to obtain a set of K orthonormal basis vectors $\mathbf{u}_1$, $\mathbf{u}_2$, ..., $\mathbf{u}_K$. If the image $f(\mathbf{x})$ lies in χ, then this transformation, f, is not useful since it brings no new information, no matter how large is the target in $f(\mathbf{x})$. This is contrary to the simple view given above. One can verify from the given images that, in general, $\mathbf{x}^n$ does not lie in χ for n>1.

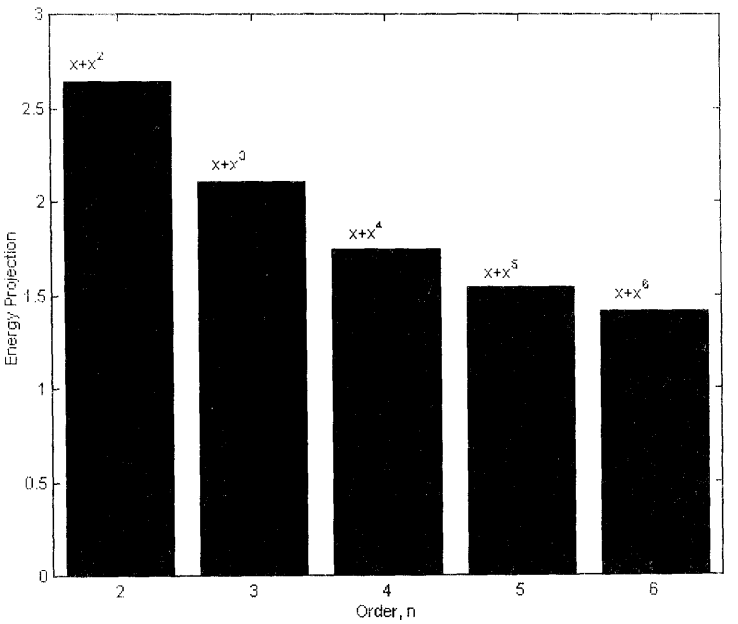

Fig. 5. Energy projection for different CPCF's.

We can write $\mathbf{x}^n$ as (see Fig. 6)

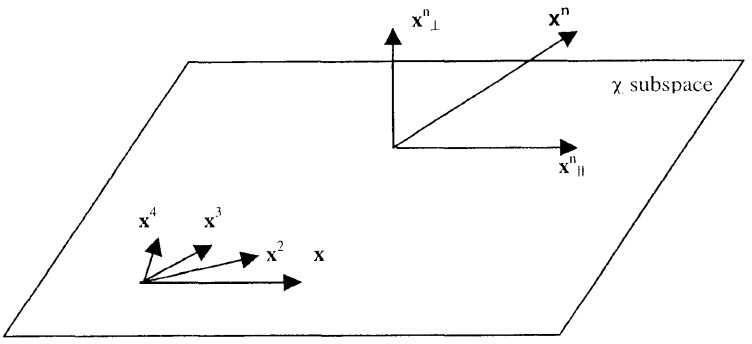

Fig. 6. Geometrical representation of $\mathbf{x}^n$ and its projections on χ subspace.

$$\mathbf{x}^n = \mathbf{x}^n_{II} + \mathbf{x}^n_\perp$$

where $\mathbf{x}^n_{II}$ is the projection of $\mathbf{x}^n$ on χ and $\mathbf{x}^n_\perp$ is its orthogonal component on χ. Therefore, we write

$$\mathbf{x}^n_{II} = \sum_{i=1}^{K} (\mathbf{u}_i^+ \mathbf{x}^n)\, \mathbf{u}_i$$

The angle, θ, between $\mathbf{x}^n$ and χ defined as

$$\theta = \cos^{-1} \frac{\left\| \mathbf{x}^n_{II} \right\|}{\left\| \mathbf{x}^n \right\|}$$

gets larger as n increases (see also Figure 6). In the same time, as explained above, the energy of the target in $\mathbf{x}^n$, after normalization by its peak, gets smaller. We propose the image energy projection to predict the significance of raising an image to the n^{th} power.

Consider χ^n, a vector subspace that is spanned by the set of all training images, say N images, raised to the n^{th} power (in one aspect bin.) We subtract from each image in χ^n its projection on χ to get the orthogonal component $\mathbf{x}^n_\perp$ defined as

$$\mathbf{x}^n_\perp = \mathbf{x}^n - \mathbf{x}^n_{II}$$

The result is a set of images, $\mathbf{x}^n_{\perp i}$, i=1...N, that are orthogonal on χ. We suggest that the energy of this orthogonal set can measure the significance of χ^n. This energy is evaluated

for each set of images in one aspect bin, and then averaged over all bins, say L bins; namely we evaluate the average energy, E, as

$$E = \frac{1}{N \times L} \sum_{i=1}^{N \times L} \left\| \mathbf{x}^{n}_{\perp i} \right\|^2$$

The result is shown in Fig. 5. We see from this figure that the energy projection follows the same trend as the signal contribution shown in Fig. 4. Higher energy projection implies higher contribution to the peak from the second filter. Thus, we can predict the significant of any term in the polynomial without computing the filter's coefficients. This handy tool needs further investigation should it be used in a general nonlinear correlation filter.

Conclusions

We presented a modified polynomial correlation filter called constrained polynomial correlation filter. We demonstrated the advantage of polynomial correlation filters through simulations on public MSTAR database. A polynomial filter consists of terms raised to different powers. In order to investigate the significance of different terms we used three approaches. In the first approach, we calculated the variance of clutter PSR. In the second one, we calculated the contribution of the second filter to the target correlation peak.

The third approach is called energy projection. We measured the significance of raising an image to the n^{th} power by computing the energy of its orthogonal component on the image's subspace. There is a high agreement between the results of these three approaches. They all suggest that the CPCF highest order should be restricted to 4 or 5. The advantage of the third approach is that it does not require computation of the actual filter. We expect that the energy projection method can be a base to establish a general theory for the evaluation of any point-by-point nonlinear filter.

References

[1] Vijaya Kumar, B.V.K. "Tutorial Survey of Composite Filter Design for Optical Correlators." *Applied Optics*, 31 (1991), 4773-4801.

[2] Hester, C.F. and Casasent, D. "Multivariant Techniques for Multiclass Pattern Recognition." *Applied Optics*, 19 (1980), 1758-1761.

[3] Mahalanobis, A., Vijaya Kumar, B.V.K. and Casasent, D. "Minimum Average Correlation Energy Filter." *Applied Optics*, 26 (1987), 3633-2640.

[4] Mahalanobis, A. Vijaya Kumar, B.V.K., Sims, S.R.F. and Epperson, j. "Unconstrained Correlation Filters." *Applied Optics*, 33 (1994), 3751-3759.

[5] Flannery, D.L. "Optimal Trade-off Distortion-tolerant Constraint-modulation Correlation Filters." *JOSA-A*, 12 (1995), 66-72.

[6] Kallman, R.R. "The Construction of Low noise Optical Correlation Filters." *Applied Optics*, 25 (1986), 1032-1033.

[7] Vijaya Kumar, B.V.K., Mahalanobis, A., Song, S., Sims, S.R.F. and Epperson, J. "Minimum Squared Error Synthetic Discnminant Functions." *Optical Engineering*, 31 (1992), 915-922.

[8] Javid, B. and Wang, J. "Design of Filters to Detect a Noisy Target in Nonoverlapping Background Noise." *JOSA-A*, 11 (1994), 2604-2612.

[9] Mahalanobis, A. and Vijaya Kumar, B.V.K. "Polynomial Filters for Higher Order Correlation and Multi-input Information Fusion." 11th Euro American Workshop, Spain, June 2-5, 1997.

[10] G. Strang, *Linear Algebra and Its Applications,* Academic Press, 1980.

[11] Hoffman, K. and Kunze, R. *Linear Algebra,* 2nd ed. Englewood Clifffs, New Jersey: Prentice-Hall, 1971.

إسقاط القدرة في مرشحات الارتباط ذات الحدود الكثيرة

خالد بن عبد العزيز المعشوق* ، ب. ف. ك. فيجاي كومار** ومحمدالكنهل**

* قسم الهندسة الكهربائية، كلية الهندسة، جامعة الملك سعود، ص.ب. ٨٠٠، الرياض ١١٤٢١، المملكة العربية السعودية
البريد الإلكتروني: mashouq @ ksu. edu. sa

** قسم هندسة الحاسب و الكهرباء، جامعة كارنيغي ميلون بتسبرغ،
ولاية بنسلفينيا ١٥٢١٣، الولايات المتحدة الأمريكية

(قُدّم للنشر في ٢٠٠٠/٦/٥م، وقبل للنشر في ٢٠٠٠/١٢/١٦م)

ملخص البحث . في هذه الورقة نعرض تعديلا جديدا على مرشح الارتباط ذي الحدود الكثيرة (PCF) اسميناه مرشح الارتباط ذي الحدود الكثيرة المقيّد (CPCF) . و قد فحصنا أداء هذا المرشح بوجود الضوضاء المنعكسة من الخلفية كما حسبنا مقياس القمة إلى الفص الجانبي لصور (MSTAR) العامة . تمّ اختبار أثر الحدود المختلفة في مرشح كثيرات الحدود بالتمثيل الحاسوبي . بعد ذلك أدخلنا إطارا نظريًا اسميناه إسقاط القدرة للتنبؤ بفعالية الحدود المختلفة في مرشح (CPCF) .